Eur Biophys J (2005) 34: 155–162
DOI 10.1007/s00249-004-0438-8

ARTICLE

Valerij F. Antonov · Andrej A. Anosov
Vladimir P. Norik · Elena Yu. Smirnova

Soft perforation of planar bilayer lipid membranes of dipalmitoylphosphatidylcholine at the temperature of the phase transition from the liquid crystalline to the gel state

Received: 13 February 2004 / Revised: 18 July 2004 / Accepted: 2 September 2004 / Published online: 5 October 2004

Abstract In contrast to the widely used method of electroporation, the method of soft perforation of lipid bilayers is proposed. It is based on the structural rearrangement of the lipid bilayer formed from disaturated phospholipids at the temperature of the phase transition from the liquid crystalline state to the gel state. This allows us to obtain a lipid pore population without the use of a strong electric field. It is shown that the planar lipid bilayer membrane (pBLM) formed from dipalmitoylphosphatidylcholine in 1 M LiCl aqueous solution exhibits the appearance of up to 50 lipid pores per 1 mm^2 of membrane surface, with an average single pore conductivity of 31 ± 13 nS. The estimation of a single pore radius carried out with water-soluble poly(ethylene glycol)s (PEGs) showed that the average pore radius ranged between 1.0–1.7 nm. It was found experimentally that PEG-1450, PEG-2000, and PEG-3350 should be in a position to block the single pore conductivity completely, while PEG-6000 fully restored the ionic conductivity. The similarity of these PEG effects to ionic conductivity in protein pores makes it possible to suggest that the partition of the PEG molecules between the pore and the bulk solution does not depend on the nature of the chemical groups located in the pore wall.

Keywords Planar lipid bilayer membrane · Soft perforation · Lipid phase transition · Electric conductance · Poly(ethylene glycol)s

V. F. Antonov (✉) · A. A. Anosov · V. P. Norik
E. Y. Smirnova
Department of Medical and Biological Physics,
Sechenov Moscow Medical Academy,
ul. B. Pirogovskaja 2/6,
119992 Moscow, Russia
E-mail: vantov@mail.ru

Introduction

Cell membrane electroporation is currently widely used in experimental biology and medicine (Lee and Hannig 2001). It is well known that electroporation is based on a reversible electrical breakdown phenomenon (Chernomordik et al. 1982). Previously we stated that a major similarity between the evolution of the lipid pores appeared in the planar lipid bilayer membrane (pBLM) both at electrical breakdown and at the membrane lipid phase transition (Antonov et al. 1985, 1992; Antonov 1998). Single lipid pores, first observed in the pBLM of distearoylphosphatidylcholine (DSPC) at the temperature of the main phase transition, demonstrated features in common with electroporation, including transformation of a hydrophobic pore into a transient hydrophilic one (Antonov et al. 1980). This result was later supported by Boheim et al. (1980) in experiments with the pBLM of the mixed-chain lipid 1-stearoyl-3-myristoyl-glycero-2-phosphocholine. From a physiological point of view, the main disadvantage of electroporation is the need for a high electrical voltage (near 230 mV) applied to the pBLM. This voltage far exceeds physiological levels. To avoid this drawback, we suggest a soft perforation procedure based on the phase transition of membrane lipids. This approach not only allows avoiding the application of high electrical voltages but it also does not need chemical pretreatment of the BLM with uranyl acetate ions, aimed at increasing the membrane matrix viscosity (Chernomordik et al. 1982).

The prime objective of this study was the experimental investigation of single lipid pore evolution induced in a pBLM by cooling at the main phase transition of synthetic zwitterionic 1,2-dipalmitoyl-*sn*-glycero-3-phosphocholine. Ionic current fluctuations were recorded at the voltage-clamp regime. The clamped voltage did not exceed 100 mV. It is shown that there is quantitative agreement between the experimentally

determined pore number in a single pBLM at soft perforation and the theoretical prediction given by the solution of appropriate equations in approximation of a zeroth membrane potential (Freeman et al. 1994). The monovalent cation selectivity study reveals the lyotropic order found earlier for the same lipid–water system by Marra and Israelashwili (1985). The poly(ethylene glycol)s (PEGs) used for the calibration of the lipid pore size were able to block conductance in the range of sizes between PEG-1450 (hydrodynamic radius 1.05 nm) and PEG-3350 (hydrodynamic radius 1.69 nm).

Materials and methods

Lipids and electrolytes

The basic membrane-forming solution contained the synthetic phospholipid 1,2-dipalmitoyl-*sn*-glycero-3-phosphocholine (Avanti). As a bulk solution, the chlorides of Li, Na, K, Rb, and Cs were used. For a probe to lipid pore radius determination, a series of PEGs was used. It included PEG-300, PEG-600, PEG-1450, PEG-3350, and PEG-6000 (Sigma). Unless otherwise specified, 20% (w/w) aqueous solutions of the PEGs were prepared.

Differential scanning calorimetry

Experiments were carried out on an adiabatic scanning microcalorimeter (DASM-4, Puschino, Russia). To prepare a sample of multilayer liposomes, the dry lipids were suspended in aqueous solutions of the appropriate chlorides by mechanical shaking on a Vortex mixer at 45 °C. Transition enthalpies were determined after measuring the area under the excess specific heat curve by paper weighing.

Planar BLMs

The planar BLMs were formed over a circular hole in a vertical wall of a Teflon pot as described by Mueller et al. (1962). The membrane-forming solution contained 25 mg of dipalmitoylphosphatidylcholine (DPPC) dissolved in 1 mL of a mixture of n-decane/chloroform/methanol (7:2:1, by volume). All experiments were performed in unbuffered aqueous solutions (pH 6.9) of the appropriate chlorides. Before each experiment the vertical wall of the Teflon pot was covered with a thin layer of the dried membrane-forming solution. To carry out experiments at constant temperature, the measuring cell was placed in a water jacket connected with a thermostat. The temperature in the cell was maintained with an accuracy ±0.5 °C. The temperature near the planar BLM was measured by a thermocouple.

Electrical measurements

The electrical capacitance changes were measured by applying a charge pulse of triangular form (in the voltage range ±50 mV) to the planar BLM and registration of the resulting cyclic current–voltage curves. The details of the measurements were made as previously described (Antonov et al. 2003). The membrane current fluctuations were recorded at voltage-clamp conditions by an ion current amplifier (Puschino, Russia).

Pore number estimation

The soft perforation procedure has some advantage over electroporation for pore number estimation. Indeed, the well-known equation for the single lipid pore energy $E(r)$ at electroporation is (Glaser et al. 1988):

$$E(r) = 2\pi\gamma r - \pi r^2\left(\sigma + \alpha U^2\right) \quad (1)$$

where r is the pore radius, γ is the edge tension of the hydrophilic pore, σ is the surface tension of the lipid bilayer, α is a coefficient dependent on the electric capacitance of the lipid bilayer, and U is the transmembrane voltage. One can see that the contribution of the surface tension at $U = 0$ and $r \to 0$ is small compared to that of the edge energy. In this case, only the first term in Eq. (1) is significant, and $E(r) \approx 2\pi\gamma r$.

This simplification seems to be quite important for the estimation of the pore number appearing in the planar BLM at steady state. According to Freeman et al. (1994), at steady-state conditions the number of lipid pores N can be evaluated as:

$$N = n_0 \lambda \exp(-r_{\min}/\lambda) \quad (2)$$

where n_0 is a constant, numerically equal to 1.2×10^{24} m^{-1}, λ is the characteristic length, and $r_{\min}$ is the minimum pore radius. The theoretical result given by Freeman et al. (1994) for the steady-state pore distribution at the non-electroporation transmembrane voltage was $N = 7$. It is essential to compare this result with the lipid pore number estimated by direct counting of uniform current fluctuations per pBLM. Of some interest is comparison of the experimental data with the conventional method based on the determination of lipid pore number by dividing the integral conductance, G_{pBLM}, of the planar BLM by the average conductance of single pore, G_{pore}:

$$N = G_{\mathrm{pBLM}}/G_{\mathrm{pore}} \quad (3)$$

Lipid pore size evaluation

At first glance, the lipid pore can be taken as being a cylindrical tube filled with electrolyte solution of ohmic

resistance. A rough estimation of the pore radius R can be obtained in this case by the equation:

$$R^2 = G_{\text{pore}} d/\pi s \quad (4)$$

where d is the thickness of the planar BLM and s is the specific conductivity of the electrolyte solution.

At the present time, the calibration of protein pores is made by PEGs of different molecular size (Krasilnikov 2001). The use of this method for lipid pores is questionable, as they are transient pores with flexible walls. Moreover, the lipid pore can be resealed owing to lateral diffusion of lipid molecules. Despite this drawback, we aimed to try this method for lipid pore size determination by taking into account the high viscosity of the lipid matrix in the gel state that might prevent the rapid resealing of the pore.

The next approach to the lipid pore size estimation is based on theoretical results obtained by Eldridge and Morowitz (1978). They suggested calibration of the pore size with a series of monovalent cations of different hydration radii. They showed that the radius R of an ohmic pore with moderate selectivity could be estimated by the equation:

$$R = a/\delta \quad (5)$$

where a is the radius of the hydrated monovalent cation and δ is a dimensionless coefficient. According to Eldridge and Morowitz (1978), the pore radius can be determined by the equation:

$$G_{\text{pore}} = g\ (\text{nanoohm}) \times \frac{J(\delta)}{1 - kK(\delta)} \quad (6)$$

where the polynomials $J(\delta)$ and $K(\delta)$ for a series of monovalent cations of different radii were tabulated by Levitt (1975). The mode of calculation of the dimensionless coefficient k and the parameter g has been described by Eldridge and Morowitz (1978).

Results

Thermograms of the BLM dispersed in monovalent cation solutions

The thermograms of the BLM from DPPC were obtained in 1 M chloride solutions of Li, Na, K, Rb, and Cs. The thermogram in Fig. 1 is typical for the DPPC endothermic phase transition, with two peaks at 35.5 °C (pretransition) and at 41 °C (main phase transition). There is no difference in the thermograms (see Fig. 1a) for all the cations listed above except for Li^+: as seen in Fig. 1b, both peaks are shifted toward higher temperature (40 °C for the pretransition and 43 °C for the main transition). The observed difference in the monovalent cations' behavior indicates that the Li^+ could be partially involved in a lipid–water interaction, strengthening the lipid bilayer (Cunningham et al. 1986).

Electric current fluctuations in the planar BLM from DPPC at the phase transition temperature

A sequence of experimental records of electric current fluctuations is shown in Fig. 2a, where a typical record is followed by the corresponding histogram. One can see that the current fluctuations at a temperature well above the phase transition are practically absent and the histogram reveals only a single peak in the vicinity of zero current. When the temperature in the experimental cell achieved the main phase transition temperature, maintained by the thermostat with an accuracy ±0.5 °C, one can see a series of single and double current fluctuations (Fig. 2b). Occasionally, threefold fluctuations have been registered. As can be seen from Fig. 2b, the duration of the current fluctuations may vary within wide limits, up to tens of seconds. The histogram reveals three distinct peaks for the current distribution at about 0, 1.5, and

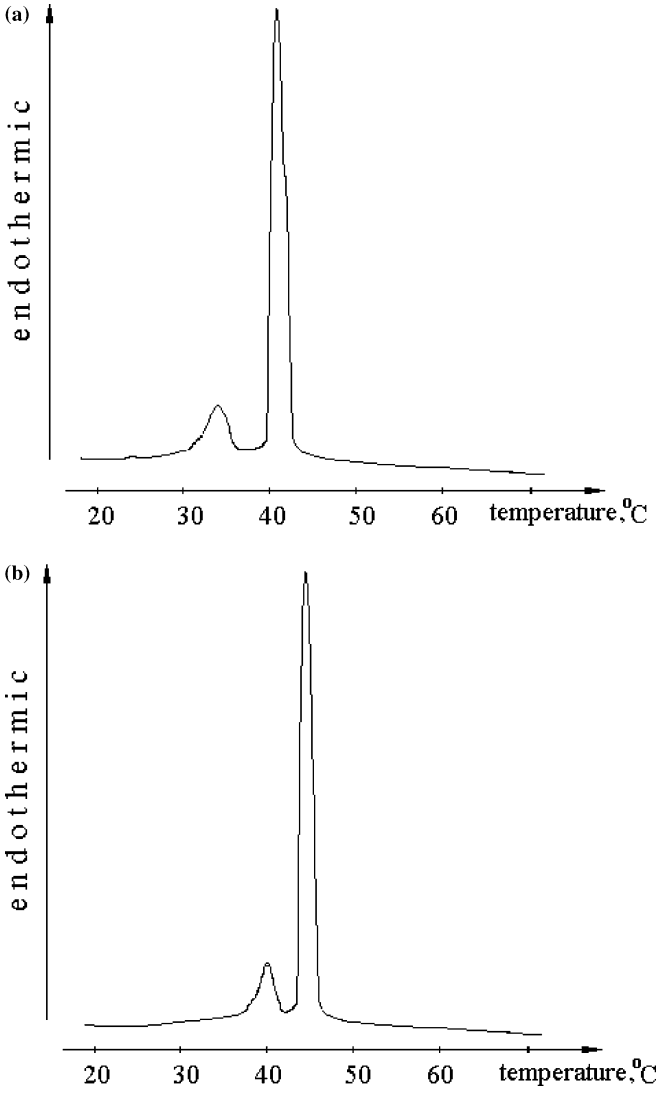

Fig. 1 Differential scanning calorimetry thermograms of the BLM from DPPC dispersed in 1 M solutions of monovalent cations (pH 6.9, without buffer): **a**, NaCl, KCl, RbCl, CsCl; **b**, LiCl

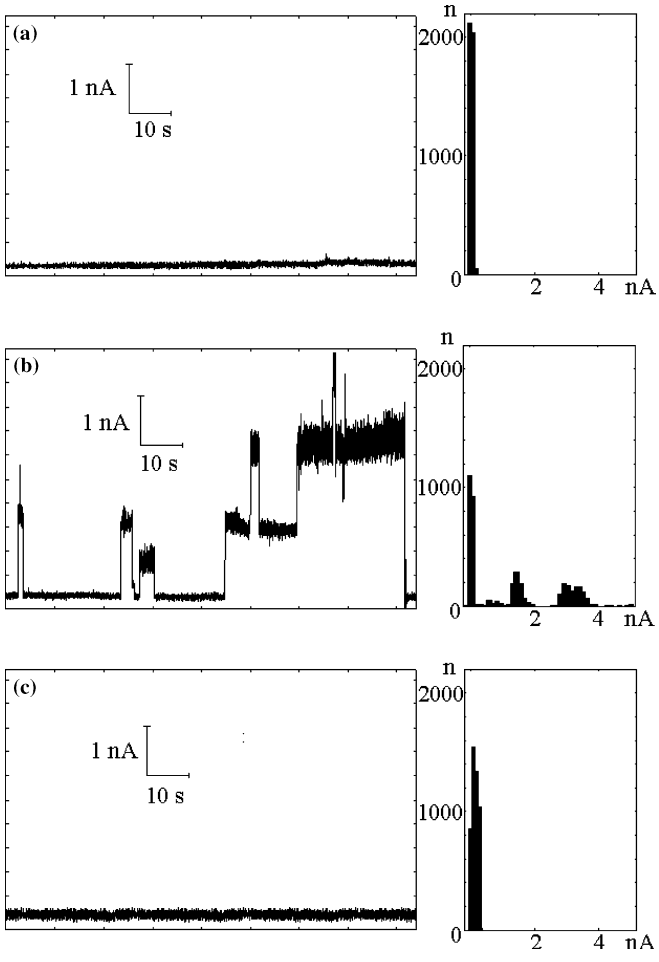

Fig. 2 Electric current fluctuations (*left*) and corresponding histograms (*right*) recorded in planar BLM from DPPC in 1 M LiCl at different temperatures: **a**, temperature above the temperature of the main phase transition of DPPC (50 °C); **b**, temperature maintained by thermostat within an accuracy of ±0.5 °C at the temperature of the main phase transition of DPPC (43 °C); **c**, temperature well below the main phase transition of DPPC (35 °C). *n* is the number of current values determined with a frequency of 80 Hz. The transmembrane potential has been clamped at 50 mV

3 nA. It should be noted that the opening of the double current fluctuation is followed by a superposition of two separate current jumps, but the closing can be followed by a single current jump. At the temperature well below the phase transition of the DPPC the resolved current fluctuations disappear and only the growth of noise is observed. It is followed by significant widening of the histogram peak at the zero level (Fig. 2c). Thus the significant current fluctuations registered at soft perforation are due to structural changes in the lipid bilayer during the phase transition of the phospholipids from the liquid crystalline state to the gel state in the relative narrow temperature interval about the temperature of the main phase transition.

Some additional data in favor of this finding have been obtained in experiments with cholesterol added to membrane-forming solutions. It is well known that cholesterol in an appropriate concentration of 30 mol% abolishes the structural rebuilding of lipid bilayers at the phase transition (Gennis 1989). The obtained data were in complete agreement with the experimental result demonstrated in Fig. 2a in all details.

The dependence of current fluctuation on the membrane low voltage

Figure 3 demonstrates typical records of the current fluctuations registered at the transition temperature by application of a clamp voltage of different amplitudes. As can be seen, the decrease of the positive voltage from +100 mV to nearly zero is followed by a reduction of the current fluctuation amplitudes. The increase of the negative clamped voltage is followed by growth of the current amplitude directed downward. The resulting voltage–current characteristic shown in the insert is linear in the range ±100 mV and passes through the origin. One can see that the conductance of a single lipid pore in 1 M LiCl solution reaches about 35 nS, which gives an indication of the existence of a relatively large pore with ohmic behavior.

Cationic selectivity of the lipid pores at soft perforation

To test the cation selectivity of the planar BLM from DPPC at soft perforation, the current–voltage curves were studied in different monovalent cation solutions. The obtained data are illustrated in Fig. 4. One can see a family of current–voltage curves separately obtained in 1 M LiCL, NaCl, KCl, RbCl, and CsCl in the voltage range of ±80 mV. It is evident that the conductance of the planar BLM of DPPC at the phase transition temperature is higher in LiCl compared to the other monovalent cations. There could be two reasons for the high lithium conductance of the planar BLM: Li^+ selectivity of single ion pores and/or a difference in the lipid pore number at soft perforation. The obtained experimental data are presented in the Table 1. Column 2 demonstrates the difference between monovalent cation conductance of single lipid pores obtained in voltage-clamp experiments. It can be seen that the cation selectivity corresponds to that given above (Fig. 4). The average lipid pore conductance in LiCl solution is greater than the average conductance of a single lipid pore in CsCl solution by a factor of three. Cation selectivity in a lipid pore at soft perforation varies only by a factor of three or so, over several monovalent alkali cations, so it is possible that electrostatic pore–solution interactions are not so important in these pores. According to the single pore conductance variations, we can arrange the selectivity order as $Li^+ \geq Na^+ > K^+ = Rb^+ \geq Cs^+$. This order in turn can be divided into two groups: Li^+ and Na^+ on the one hand and K^+, Rb^+, and Cs^+ on the other. The results are in good agreement with the classification derived by Kraayenhof et al. (1996). They suggested that monovalent

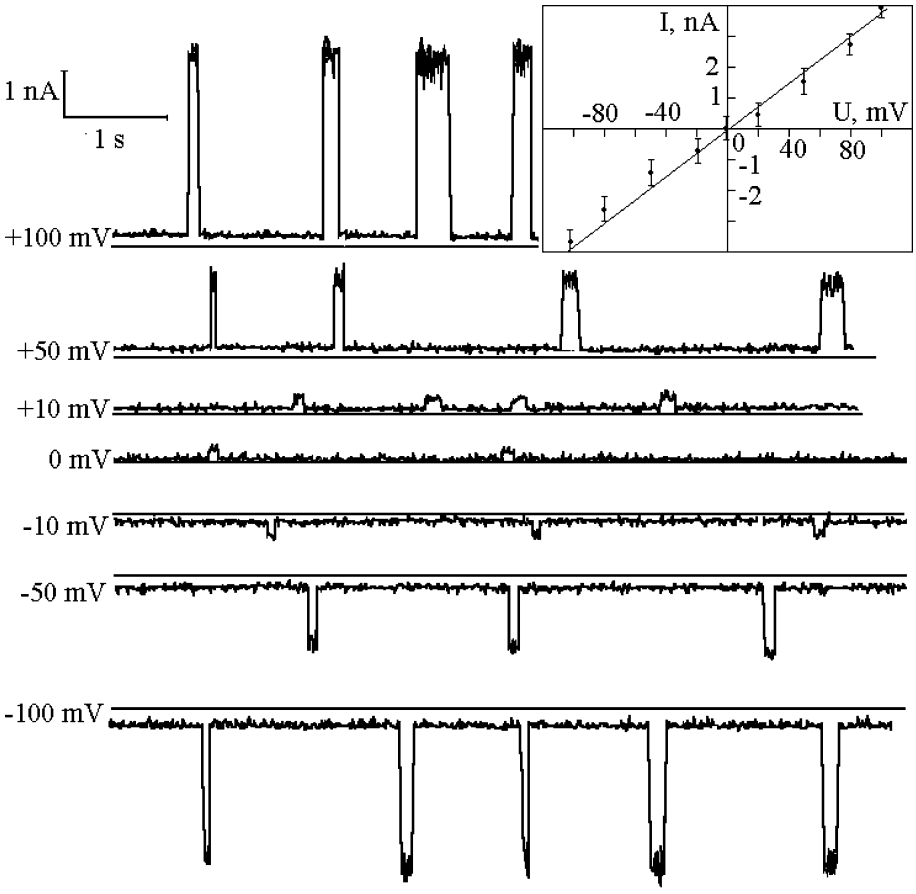

Fig. 3 Current fluctuations in the planar BLM from DPPC at the temperature of the main phase transition (43 ± 0.5 °C) determined at different clamp voltages. *Horizontal lines* correspond to zero level. The medium contained 1 M LiCl, pH 6.9, without added buffer. The *insert* demonstrates typical current–voltage characteristics of a single pore averaged over 150 experimental points

cations may perturb the hydration layer of the BLM, and thereby the membrane stability, to different extents, depending on their own hydration tendency. Among the alkali metal ions, Li^+ and Na^+ belong to the group of so-called water "structure makers". In contrast, K^+, Rb^+, and Cs^+ are called water "structure breakers". This is consistent with the idea that the hydration force (distinct from electrostatic force) is responsible for the observed cation selectivity of the planar BLM at soft perforation.

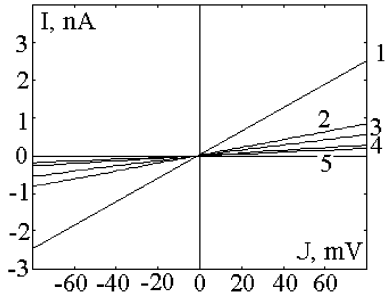

Fig. 4 Current–voltage characteristics of the planar BLM from DPPC recorded for different monovalent cations (1 M) at appropriate temperatures of the main phase transition: *1*, LiCl; *2*, NaCl; *3*, KCl; *4*, RbCl; *5*, CsCl. The pH of each solution was 6.9, without added buffer

Lipid pore size estimation

As mentioned above, three independent ways of pore size estimation have been used. The simplest form is based on single pore conductance data according to Eq. (4). The second approach is based on a hydrodynamic theory of ion conductance through ohmic pores (Eldridge and Morowitz 1978). This latter approach is highly suitable for our data because of ohmic conductance and moderate cationic selectivity. When both the channel conductance and the ion size are known, the radius of the channel may be estimated (Eq. 5). The third method relies upon the effect of symmetrically applied polymeric non-electrolyte PEGs on the pore conductance to estimate the pore size. As far as we know, this method has not been applied to lipid pore size determination before.

The obtained data are summarized in Table 1. The data collected in the fourth column were obtained by calculation with Eq. (4). The data reflect, to some extent, the moderate selectivity within the monovalent cations. It is seen that the radius of a Li^+ pore (2.1 nm) is over twice as large as that for a Cs^+ pore (0.9 nm). The fifth column represents data calculated by Eq. (5). The method of calculation is derived by equating the electrical force on the ion (the driving force) with the frictional force against the motion of the ion (the dissipative force). This approach has been successfully employed

Table 1 Average electric conductance of single lipid pores, sizing of single lipid pore radius and lipid pore number in the planar BLM from DPPC at the main phase transition temperature. Medium contained 1 M chlorides of Li^+, Na^+, K^+, Rb^+, Cs^+; pH 6.9

Cation	Lipid pore conductance (nS) (experimental)[a]	Lipid pore radius (nm) size by			Lipid pore number	
		PEG molecules (experimental)	Eq. (<equationcite> 4 </equationcite>)	Eq. (<equationcite> 5 </equationcite>)[c]	Estimated by counting[d] the current fluctuation per one BLM[e] (experimental)	Calculated by Eq. (<equationcite> 3 </equationcite>)
Li^+	31 ± 15 (250)	1.05[b] (PEG-1440) 1.22 (PEG-2000) 1.69 (PEG-3550)	2.1	1.4	36 ± 7 (7)	~1
Na^+	28 ± 16 (90)	–	1.9	1.5	12 ± 5 (7)	~0.5
K^+	12 ± 2 (80)	–	1.0	1.4	10 ± 4 (7)	< 0.5
Rb^+	12 ± 4 (50)	–	1.0	1.3	7 ± 3 (6)	< 0.5
Cs^+	10 ± 6 (40)	–	0.9	1.3	4 ± 2 (8)	< 0.5
	Average	1.3 ± 0.3		1.4 ± 0.1		

[a]Numbers in parentheses indicate the number of single lipid pores in sample
[b]Hydrodynamic radius of PEG molecules blocking single lipid pore conductance (nm)
[c]Polynomials $J(\delta)$ and $K(\delta)$ for monovalent cations are: Li^+ (ion hydration radius $a = 0.237$ nm), $\delta = 0.166$, $J = 0.44$, $K = 24.8$, $k = 0.038$, $g = 4.6$ nS; Na^+ ($a = 0.183$ nm), $\delta = 0.123$, $J = 1.00$, $K = 50.3$, $k = 0.017$, $g = 3.56$ nS; K^+ ($a = 0.125$ nm), $\delta = 0.09$, $J = 2.2$, $K = 101.7$, $k = 0.006$, $g = 2.43$ nS; Rb^+ ($a = 0.11$ nm), $\delta = 0.08$, $J = 2.921$, $K = 131.7$, $k = 0.004$, $g = 2.14$ nS; Cs^+ ($a = 0.119$ nm), $\delta = 0.09$, $J = 2.2$, $K = 101.7$, $k = 0.005$, $g = 2.3$ nS (from Eldridge and Morowitz 1978)
[d]Only for current impulses, the amplitudes of which were three times greater than the noise level
[e]Tested BLM number. The lifetime of planar BLMs has been assumed as equal

for alamethicin pore size evaluation (Eldridge and Morowitz 1978). One can see that the data given in column 4 are concentrated around the pore radius (1.4 nm), which is close to that shown above (column 5). The difference between them consists of the absence of any ion selectivity in the latter case.

Calibration of Li^+ pores with water-soluble PEGs

The experimental data are reproduced in Fig. 5. The first record demonstrates the current fluctuations in the planar BLM of DPPC at a clamp voltage of 50 mV, measured at the temperature of the main phase transition of DPPC without PEG (see, for comparison, Fig. 2b). In subsequent experiments (Fig. 5b–g), the membrane-bathing solution was substituted for 20% (w/w) solutions of differently sized PEGs. The successive additions of PEG-300 (Fig. 5b) and PEG-600 (Fig. 5c) are followed by a gradual decrease of current fluctuation amplitudes and by a lowering of the current fluctuation number. In solutions of PEG-1450, PEG-2000, and PEG-3350 the current fluctuations disappear completely (Fig. 5d–f), but the addition of PEG-6000 (Fig. 5g) is followed by nearly full restoration of electrical activity of the planar BLM. We treat the obtained data in such a way that initially the electric current through the lipid pores is carried mainly by Li^+. The addition to the solution of PEG-300 and PEG-600 is followed by local penetration of electrically neutral polymer molecules into the pore and by subsequent lowering of the transmembrane electric current. In solutions of PEG-1450, PEG-2000, and PEG-3350 the electric current through the lipid pores is nearly completely blocked. The larger sized PEG-6000 probably does not penetrate the planar BLM at all. It is seen that the large, presumably excluded, PEG-6000 practically does not change the ionic current through the pore. In conclusion, it should be noted that solute exclusion experiments widely used to evaluate the size of protein pores could be extended to include pure lipid pores at electroporation and soft perforation. It is seen (see column 3 in Table 1) that the average pore radius of 1.3 nm found by the solute exclusion method is in reasonably good agreement with the data given by other methods.

Lipid pore number

One essential feature of the soft perforation mechanism is the lack of a high transmembrane voltage needed for membrane breakdown at electroporation. In the latter case, the high voltage is responsible for the appearance of more than 10^5 lipid pores at once (Chernomordik et al. 1982). The initial number of lipid pores at $U = 0$ V could be determined in this case only by extrapolation, although this result has long been a subject of contention (Wilhelm et al. 1993). Therefore it would be rea-

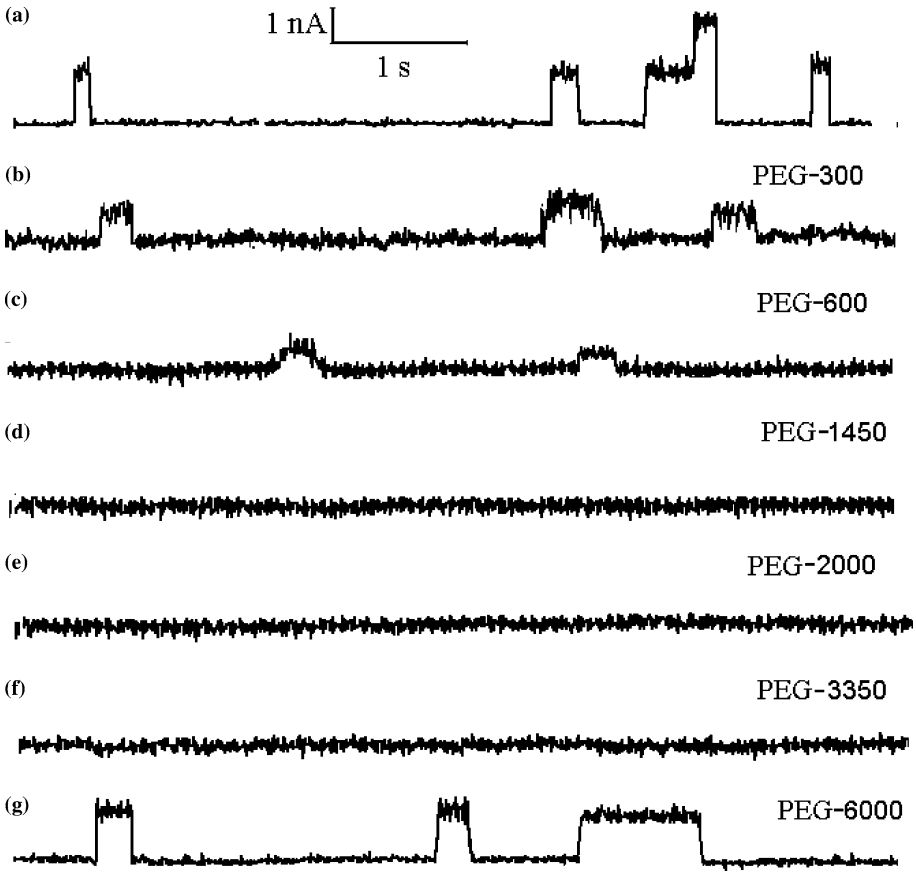

Fig. 5 Current fluctuations in the planar BLM from DPPC at a voltage clamped at 50 mV in 1 M LiCl after addition of 20% PEGs of different molecular size: *a*, without added PEG; *b*, PEG-300; *c*, PEG-600; *d*, PEG-1450; *e*, PEG-2000; *f*, PEG-3350; *g*, PEG-6000

sonable to obtain experimental data about lipid pore numbers at small non-breakdown transmembrane voltages. The experimental data are shown in the Table 1 (column 6). Generally, it is seen that the lipid pore number is very small compared to that appearing at electroporation. Moreover, the pore number calculated by Eq. (3) is nearly equal or less than 1 (column 7). Surprisingly, there is good agreement between the pore number predicted by theory (Eq. 2) and that experimentally determined for all monovalent cations. These good correlations point to the fact that the phase transition of the lipid in the planar BLM to the gel state has not been followed by creation of additional pore numbers comparable to statistically distributed pores due to thermal fluctuations. The effect of the phase transition into the gel state likely amounts to a retardation of the pore resealing process that prolongs the pore lifetime.

Discussion

In contrast to electroporation, the soft perforation of membranes does not need the application of a high transmembrane voltage. Beyond the evident practical interest, this peculiarity could be very useful for discussion of the theoretical background of the perforation mechanism. In the planar BLM at $U=0$ V we can neglect the surface tension σ in the determination of the pore radius distribution (see Eq. 1). In this case the pore edge tension γ remains as a single parameter determining the pore number (Freeman et al. 1994). Our experimental results are in reasonably good agreement with the theoretical prediction of the lipid pore number detected by Freeman et al. As a matter of fact, this result is a confirmation of the relative independence between γ and σ predicted earlier by Petrov et al. (1982). They showed that, even in the tension-free case in the planar lipid bilayer, $\gamma > 0$. This is due to the fact that in the curved part of the monolayer inside the pore, the tension is always non-zero. This approach seems to be fruitful for the explanation of the experimentally observed lipid pore appearance in a tension-free liposome membrane at the phase transition $L_\alpha \rightarrow L_\beta$ (Jacobson and Papahadjopoulos 1975, Evans and Kwok 1982).

Hydrophobic and hydrophilic lipid pores are involved in the planar BLM permeabilization at soft perforation. The relationship between them can be established by comparing the lipid pore number observed experimentally with that estimated by calculation. Taking into account the known data from X-ray examination of the area per one lipid molecule in the bilayer at the phase transition $L_\alpha \rightarrow L_\beta$ (0.58 nm^2 and 0.48 nm^2 for DPPC, respectively) (Gennis 1989), we can estimate the overall area occupied by hydrophobic pores in 1 mm^2 of planar BLM as 0.17×10^{12} nm^2. The radius of a single hydrophilic pore can be estimated as $R \geq 1/2\times d$, where d is the thickness of the planar BLM. The rough estimation of the hydrophobic pore number gives

approximately 10^{10} pores per 1 mm^2. Comparing this number with that given in Table 1, we can conclude that the pores under investigation comprise a vanishingly small part of the hydrophobic pore number at the transition $L_\alpha \rightarrow L_\beta$. Therefore we can suggest that the pores obtained in the study belong to the type of hydrophilic pores analyzed by Freeman et al. (1994). Three groups of data obtained in our experiments evidence the hydrophilic nature of the pores under consideration: the good agreement in pore size determination based on hydrophilic pore approximation, the selectivity of lipid pore conductance for some of the hydrated monovalent cations (Fig. 4), and the dependence of pore conductance on the size of hydrated PEGs.

The evident similarity in the effects of the PEG on the electric conductance of the lipid pores at soft perforation and protein pores (Rostovtseva et al. 2002) has been elucidated. It includes a number of phenomenological effects such as the dependence of the pore conductance on PEG molecule size (Fig. 5), the availability of a "cutoff" polymer size (Fig. 5), and the blockade of lipid pore conductance by PEGs with molecular sizes of 1.05–1.69 nm (see column 3 in Table 1). It is evident therefore that the effect of PEG on a single pore conductance does not depend upon the chemical nature of the molecules covering the pore wall surface.

Acknowledgements We thank Prof. G. N. Berestovskij for helpful and stimulating discussions. This work was supported partially by a grant from the Russian Fund for Basic Research.

References

Antonov VF (1998) Lipid pores: stability and permeability of the membrane (in Russian). Soros Educ J 10:10–17

Antonov VF, Petrov VV, Molnar AA, Predvoditelev DA, Ivanov AS (1980) The appearance of single ion channels in unmodified lipid bilayer membrane at the phase transition temperature. Nature 283:585–588

Antonov VF, Shevchenko EV, Kozhomkulov ET, Molnar AA, Smirnova EYu (1985) Capacitance and ion currents in BLM from phosphatidic acids in Ca^{2+} induced phase transition. Biochem Biophys Res Commun 133:1098–1103

Antonov VF, Smirnova EYu, Shevchenko EV (1992) Lipid membranes at the phase transition (in Russian). Moscow, Nauka, pp 1–135

Antonov VF, Anosov AA, Norik VP, Korepanova EA, Smirnova EYu (2003) Electrical capacitance of lipid bilayer membrane of hydrogenated egg lecithin at the temperature phase transition. Eur Biophys J 32:55–59

Boheim G, Hanke W, Eibl H (1980) Lipid phase transition in planar lipid membrane and its effect on carrier- and pore-mediated ion transport. Proc Natl Acad Sci USA 77:3403–3407

Chernomordik LV, Sukharev IS, Abidor IG, Chismadzhev YuA (1982) The study of the BLM reversible electrical breakdown mechanism in the presence of UO_2^{2+}. Bioelectrochem Bioenerg 6:149–165

Cunningham BA, Shimotake JE, Tamura-Lis W, Mastran T, Kwok JT, Kaufman JW, Lis LJ (1986) The influence of ion species on phosphatidylcholine bilayer structure and packing. Chem Phys Lipids 39:135–143

Eldridge CA, Morowitz HJ (1978) A hydrodynamic theory of ion conductance through ohmic pores. J Theor Biol 73:539–548

Evans E, Kwok R (1982) Mechanical calorimetry of large dimyristoylphosphatidylcholine vesicles in the phase transition region. Biochemistry 21:4874–4879

Freeman SA, Wang MA, Weaver JC (1994) Theory of electroporation of planar bilayer membranes: predictions of aqueous area, change in capacitance and pore-pore separation. Biophys J 67:42–56

Gennis R (1989) Biomembranes. Molecular structure and function. Springer, Berlin, Heidelberg, New York

Glaser RW, Leikin SL, Chernomordik LV, Pastushenko VF, Sokirko AV (1988) Reversible electrical breakdown of lipid bilayers: formation and evolution of pores. Biochim Biophys Acta 940:275–287

Jacobson K, Papahadjopoulos D (1975) Phase transitions and phase separations in phospholipid membranes induced by changes in temperature, pH and concentration of bivalent ions. Biochemistry 14:152–161

Kraayenhof R, Sterk GJ, Harro W, Wong FS, Krab K, Epand RM (1996) Monovalent cations differentially affect membrane surface properties and membrane curvature, as revealed by fluorescent probes and dynamic light scattering. Biochim Biophys Acta 1282:293–302

Krasilnikov OV (2001) Sizing channels with polymers. In: Kasianowicz JJ, Kellermayer MSZ, Deamer DV (eds) Structure and dynamics of confined polymers. Kluwer, Dordrecht, The Netherlands, pp 73–91

Lee RC, Hannig J (2001) Membrane biology and biophysics. Surgical Res 25:297–305

Levitt DG (1975) General continuum analysis of transport through pores. II. Nonuniform pores. Biophys J 15:553–563

Marra J, Israelashwili J (1985) Direct measurements of forces between phosphatidylcholine and phosphatidylethanolamine bilayers in aqueous electrolyte solutions. Biochemistry 24:4608–4618

Mueller P, Rudin D, Tien H, Wescott W (1962) Reconstruction of cell membrane structure in vitro and its transformation into an excitable system. Nature 194:979–980

Petrov AC, Mitov AD, Derzhanski AJ (1982) Edge energy and pore stability. In: Bata I (ed) Advances in liquid crystal research and applications, vol 2. Pergamon, Oxford, UK, pp 695–737

Rostovtseva TK, Nesterovich EM, Bezrukov SM (2002) Partitioning of differently sized poly(ethylene)glycols into OMPF porin. Biophys J 82:160–169

Wilhelm C, Winterhalter M, Zimmermann U, Benz R (1993) Kinetics of pore size during irreversible electrical breakdown of lipid bilayer membranes. Biophys J 64:121–128